Appl. Math. Mech. -Engl. Ed., **41**(8), 1269–1286 (2020)

APPLIED MATHEMATICS AND MECHANICS (ENGLISH EDITION)

https://doi.org/10.1007/s10483-020-2635-7

Vibration suppression of magnetostrictive laminated beams resting on viscoelastic foundation*

A. M. ZENKOUR[1,2,†], H. D. EL-SHAHRANY[1,3]

1. Department of Mathematics, Faculty of Science, King Abdulaziz University, Jeddah 21589, Saudi Arabia;
2. Department of Mathematics, Faculty of Science, Kafrelsheikh University, Kafrelsheikh 33516, Egypt;
3. Department of Mathematics, Faculty of Science, Bisha University, Bisha 61922, Saudi Arabia

(Received Mar. 31, 2020 / Revised Apr. 22, 2020)

Abstract The vibration suppression analysis of a simply-supported laminated composite beam with magnetostrictive layers resting on visco-Pasternak's foundation is presented. The constant gain distributed controller of the velocity feedback is utilized for the purpose of vibration damping. The formulation of displacement field is proposed according to Euler-Bernoulli's classical beam theory (ECBT), Timoshenko's first-order beam theory (TFBT), Reddy's third-order shear deformation beam theory, and the simple sinusoidal shear deformation beam theory. Hamilton's principle is utilized to give the equations of motion and then to describe the vibration of the current beam. Based on Navier's approach, the solution of the dynamic system is obtained. The effects of the material properties, the modes, the thickness ratios, the lamination schemes, the magnitudes of the feedback coefficient, the position of magnetostrictive layers at the structure, and the foundation modules are extensively studied and discussed.

Key words vibration suppression, laminated composite beam, magnetostrictive material, visco-Pasternak's foundation

Chinese Library Classification O343
2010 Mathematics Subject Classification 74G60

1 Introduction

In the 19th century, a special effect of ferromagnetic material was discovered by English physicist James Joule, which is called the "Joule effect". The term "magnetostriction" was used to describe this effect as a change in the physical shape or size of the material in response to the action of magnetic forces (the applied magnetic field). Magnetostrictive materials are very common to be utilized as actuators and sensors where these materials are appropriate for providing giant forces, strains, high energy densities, noise, and vibration control for

* Citation: ZENKOUR, A. M. and EL-SHAHRANY, H. D. Vibration suppression of magnetostrictive laminated beams resting on viscoelastic foundation. *Applied Mathematics and Mechanics* (*English Edition*), **41**(8), 1269–1286 (2020) https://doi.org/10.1007/s10483-020-2635-7

† Corresponding author, E-mail: zenkour@kau.edu.sa

heavy structures. First, in smart laminated structure applications, it is necessary to study the interactions between the laminated composites and the magnetostrictive layers. To understand more about the background of the topic, some articles about magnetostrictive materials and laminated composite structures are introduced in this part. Reddy[1] presented an analysis of laminated fiber-reinforced composite beams/plates/shells with/without layers of smart materials extensively. Some researchers have especially introduced some designing and theoretical studies about magnetostrictive materials and active control of beams, plates, and shells with magnetostrictive layers[2–16]. Lee and Reddy[17] analyzed the non-linear response of magnetostrictive laminated plate subjected to thermo-mechanical load using the finite element method. Reddy[18] also presented and discussed a linear model of thick laminated composites with integrated sensors and actuators by using his third-order plate theory. Zenkour[19] presented the exact solutions for torsional analysis of heterogeneous magnetostrictive circular cylinder under the effect of a magnetic field where the cylinder rigidity was graded through the axial direction of the cylinder using two materials from the lower base to the upper base. Zhang et al.[20] presented a nonlinear model to study the active vibration control of a cantilever laminated composite plate embedded giant magnetostrictive material layers. The model was used to show the inherent and complicated nonlinearities of giant magnetostrictive materials in response to the magnetic field under partiality conditions (pre-stress and bias magnetic field).

Terfenol-D is the most commercially obtainable magnetostrictive material as well as the most commonly used engineering magnetostrictive material for actuator applications, typical transducers, and magnetostrictive motors. Many studies have discussed the material properties of dynamic and static applications for Terfenol-D[21–22]. In addition, Anjanappa and Bi[23–24] discussed the feasibility of smart structural applications, which embeds Terfenol-D mini actuators. Besides, the mechanical response of smart structures is affected via the coupling between mechanical and magnetic impacts. Zenkour and El-Shahrany[25] presented a theoretical study of vibration response of laminated composite beams embedded with four layers of Terfenol-D material with simply-supported boundary conditions according to the hyperbolic shear deformation beam theory. Also, Zenkour and El-Shahrany[26] developed the pervious theoretical study to include the smart plates considering the shear and normal deformations influences. Moreover, the composite plate and shell shapes have been controlled using actuators by Koconis et al.[27].

Several studies have also analyzed the vibration behaviors of smart beam/plate undergoes some situations and effects such as thermal effect, hygrothermal environment, elastic foundation, certain types of loading, and external forces. Hong[28–29] utilized the generalized differential quadrature (GDQ) method to study the thermal vibration behavior of magnetostrictive material in thin and thick rectangular laminated plates with and without the shear effect under the simply-supported boundary conditions. Shankar et al.[30] presented the study of vibration control for composite plates embedded sensor and actuators with delamination under the hygrothermal effect. Arani and Maraghi[31] studied the vibration behavior of the magnetostrictive smart plate (MSP) under an external follower force. Arani et al.[32] also discussed the free vibration of a rectangular magnetostrictive plate subjected to in-plane forces in the x- and y-directions and supported by the elastic medium as Pasternak's foundation utilizing a trigonometric higher-order shear deformation theory.

The viscoelastic foundation effect has been used in the present work, and various papers are introduced in this field[33–38]. Baferani and Saidi[39] used a third-order shear deformation plate theory to present an exact analytical solution for the vibration and buckling of thick rectangular laminated plates on the elastic foundation under various in-plane loadings. Malekzadeh et al.[40] utilized the Lindstedt-Poincare perturbation technique to find a solution vibration problem for laminated plates on the elastic foundation under non-ideal boundary conditions and initial stress in-plane loads. Thai et al.[41] anticipated a simple refined shear deformation theory to study the vibration, buckling, and bending of thick rectangular plates supported by

Pasternak's foundation with two opposite edges having arbitrary boundary conditions and the other simply-supported edges. Razavi and Shooshtari[42] investigated the impacts of the electric and magnetic potentials, Pasternak's foundation parameters on the free vibration of a magneto-electro-elastic doubly-curved thin shell supported by Pasternak's foundation according to the Donnell theory and the simply-supported boundary condition. Zamani et al.[43] found a solution for the transient response of laminated viscoelastic composite plates on Pasternak viscoelastic medium by a weighted residual method with simply-supported edge conditions according to a third-order shear deformation theory.

In this work, the vibration of a laminated composite beam with two layers of Terfenol-D particles embedded in a visco-Pasternak's medium has been investigated. Perfect orientation and zero pre-stress layers are assumed in the magnetostrictive layers. The simple feedback control of velocity is utilized. The theory of unified shear deformation along with the sinusoidal shear deformation beam theory is used[44–49]. The governing dynamic equations are solved for a simply-supported boundary condition analytically. The deflection damping characteristics are discussed, and the effects of some different parameters on the vibration suppression are discussed, tabulated, and graphically illustrated to help other investigators with their future treatments.

2 Theoretical model

Let us consider a symmetric laminated composite beam of kth layers with total thickness h and length L. The current beam contains two magnetostrictive layers made of Terfenol-D particles embedded in resin. The smart material is located in mth and $(k-m+1)$th layers, and the residual $(k-2)$ layers are made of fiber-reinforced materials. The structure is embedded in a homogeneous three-parameter viscoelastic medium (see Fig. 1). The simple sinusoidal shear deformation beam theory, Euler-Bernoulli's beam theory, Timoshenko's first-order, and Reddy's third-order beam theories are utilized to analyze the system as special cases of the used unified shear deformation theory. To simplify the development of all four theories in a united approach, the displacement field components are represented as follows:

$$\begin{cases} u(x,y,z,t) = f_1(z)\dfrac{\partial w_0}{\partial x} - f_2(z)\varphi(x,t), \\ v(x,y,z,t) = 0, \\ w(x,y,z,t) = w_0(x,t). \end{cases} \tag{1}$$

The above displacement field contains only two unknown functions w_0 and φ, where w_0 denotes the transverse displacement (deflection) at $z = 0$, and $\varphi(x,t)$ is the rotation of a transverse normal line. The functions $f_1(z)$ and $f_2(z)$ are given as follows:

$$f_1(z) = -c_0 z - c_2 z^3, \quad f_2(z) = c_1 e(z) - c_2 z^3. \tag{2}$$

The field of displacement in Eq. (1) can be displayed according to different beam theories as follows.

Euler-Bernoulli's classical beam theory (ECBT):

$$c_0 = 1, \quad c_1 = c_2 = 0.$$

Timoshenko's first-order beam theory (TFBT):

$$c_0 = 0, \quad c_1 = 1, \quad c_2 = 0, \quad e(z) = z.$$

Reddy's higher-order beam theory (RHBT):

$$c_0 = 0, \quad c_1 = 1, \quad c_2 = 4/(3h^2), \quad e(z) = z.$$

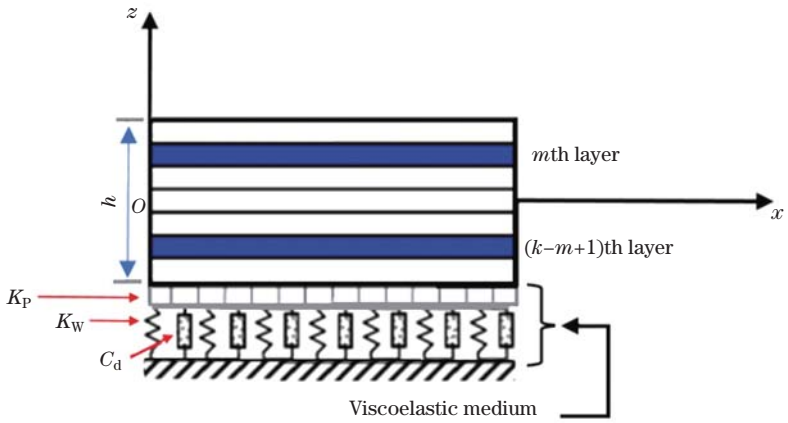

Fig. 1 Schematic diagram of the structure

Simple sinusoidal beam theory (SSBT):

$$c_0 = c_1 = 1, \quad c_2 = 0, \quad e(z) = \frac{h}{\pi}\sin\Big(\frac{\pi z}{h}\Big).$$

The strain-displacement components are determined as follows:

$$\begin{cases} \varepsilon_{xx} = f_1(z)\dfrac{\partial^2 w_0}{\partial x^2} + f_2(z)\dfrac{\partial \varphi}{\partial x} = z\varepsilon_{xx}^{(1)} + z^3\varepsilon_{xx}^{(3)} + e(z)\varepsilon_{xx}^{e}, \\ \gamma_{xz} = (1-c_0)\dfrac{\partial w_0}{\partial x} + c_1 g(z)\varphi - 3c_2 z^2\Big(\varphi + \dfrac{\partial w_0}{\partial x}\Big) \\ \qquad = \gamma_{xz}^{(0)} + g(z)\gamma_{xz}^{g} + z^2\gamma_{xz}^{(2)}, \end{cases} \tag{3}$$

where

$$\begin{cases} \varepsilon_{xx}^{(1)} = -c_0\dfrac{\partial^2 w_0}{\partial x^2}, \quad \varepsilon_{xx}^{(3)} = -c_2\Big(\dfrac{\partial^2 w_0}{\partial x^2} + \dfrac{\partial \varphi}{\partial x}\Big), \\ \varepsilon_{xx}^{e} = c_1\dfrac{\partial \varphi}{\partial x}, \quad \gamma_{xz}^{(0)} = (1-c_0)\dfrac{\partial w_0}{\partial x}, \\ \gamma_{xz}^{g} = c_1\varphi, \quad \gamma_{xz}^{(2)} = -3c_2\Big(\varphi + \dfrac{\partial w_0}{\partial x}\Big), \quad g(z) = e'(z). \end{cases} \tag{4}$$

The stress-strain relationships of the kth fiber-reinforced layer are given by

$$\sigma_{xx}^{(k)} = \overline{Q}_{11}^{(k)}\varepsilon_{xx}, \quad \sigma_{xz}^{(k)} = \overline{Q}_{55}^{(k)}\gamma_{xz}. \tag{5}$$

Also, the stress-strain relation of the magnetostrictive layer is represented by

$$\sigma_{xx}^{(m)} = \overline{Q}_{11}^{(m)}\varepsilon_{xx} - \overline{q}_{31}^{(m)}H_z. \tag{6}$$

The coefficients $\overline{Q}_{11}^{(k)}$ and $\overline{q}_{31}^{(m)}$ are given in Appendix A, where $\overline{Q}_{11}^{(k)}$ are the transformed plane stress-reduced stiffnesses, $\overline{q}_{31}^{(m)}$ is the transformed magnetostrictive modulus, and H_z denotes the component of the magnetic field intensity in the z-direction.

According to the simple feedback control of velocity, the relationship between the intensity of the magnetic field H_z and the coil current $I(x,t)$ can be defined as

$$H_z(x,t) = k_c I(x,t), \tag{7}$$

in which

$$k_{\mathrm{c}}=\frac{n_{\mathrm{c}}}{\sqrt{(b_{\mathrm{c}}^2+4r_{\mathrm{c}}^2)}},\quad I(x,t)=c(t)\frac{\partial w}{\partial t},\tag{8}$$

where k_{c}, b_{c}, r_{c}, and n_{c} are the coil constant, the coil width, the coil radius, and the number of turns in the coil, respectively. Moreover, $c(t)$ represents the control gain.

3 Governing equations

By applying Hamilton's principle, the equations of motion are deduced as

$$\delta\int_0^t(U+V-K)\mathrm{d}t=0,\tag{9}$$

where K, U, and V are, respectively, the kinetic energy, the strain energy, and the work done by the external loads. Therefore, the virtual strain, the kinetic energies, and the virtual work due to the surrounding visco-Pasternak's medium of the beam are obtained as

$$\begin{cases}\delta U=\displaystyle\int_0^L\int_{-h/2}^{h/2}\big(\sigma_{xx}\big(z\delta\varepsilon_{xx}^{(1)}+z^3\delta\varepsilon_{xx}^{(3)}+e(z)\delta\varepsilon_{xx}^{e}\big)\\ \qquad+\sigma_{xz}\big(\gamma_{xz}^{(0)}+g(z)\gamma_{xz}^{g}+z^2\gamma_{xz}^{(2)}\big)\big)\mathrm{d}z\mathrm{d}x,\\ \delta V=-\displaystyle\int_0^L(q-E_{\mathrm{f}})\delta w_0\mathrm{d}x,\quad E_{\mathrm{f}}=K_{\mathrm{W}}w_0-K_{\mathrm{P}}\frac{\partial^2 w_0}{\partial x^2}+c_{\mathrm{d}}\frac{\partial w_0}{\partial t},\end{cases}\tag{10}$$

where c_{d}, K_{W}, and K_{P} are the damper parameter, the Winkler's spring modulus, and the shear foundation parameters, respectively.

$$\delta K=\int_0^L\int_{-h/2}^{h/2}\rho\Big(f_1\Big(\frac{\partial\dot{w}_0}{\partial x}+f_2\dot{\varphi}\Big)\Big(f_1\frac{\partial\delta\dot{w}_0}{\partial x}+f_2\delta\dot{\varphi}\Big)+\dot{w}_0\delta\dot{w}_0\Big)\mathrm{d}z\mathrm{d}x.\tag{11}$$

By using the integral by parts, we obtain the following equation:

$$\begin{aligned}0=\int_0^T\int_0^L\Big(&M_{xx}\delta\varepsilon_{xx}^{(1)}+P_{xx}\delta\varepsilon_{xx}^{(3)}+S_{xx}\delta\varepsilon_{xx}^{e}+Q_x\delta\gamma_{xz}^{(0)}+Q_g\delta\gamma_{xz}^{g}\\&+R_x\delta\gamma_{xz}^{(2)}-(q-E_{\mathrm{f}})\delta w_0-\Big(K_1\frac{\partial\dot{w}_0}{\partial x}+K_3\dot{\varphi}\Big)\frac{\partial\delta\dot{w}_0}{\partial x}\\&-\Big(K_3\frac{\partial\dot{w}_0}{\partial x}+K_2\dot{\varphi}\Big)\delta\dot{\varphi}-I_0\dot{w}_0\delta\dot{w}_0\Big)\mathrm{d}x\mathrm{d}t.\end{aligned}\tag{12}$$

In the final form, the equation becomes the following expression:

$$\begin{aligned}0=\int_0^T\int_0^L\Big(\Big(&-c_0\frac{\partial^2M_{xx}}{\partial x^2}-c_2\Big(\frac{\partial^2P_{xx}}{\partial x^2}-3\frac{\partial R_x}{\partial x}\Big)-(1-c_0)\frac{\partial Q_x}{\partial x}-q\\&+E_{\mathrm{f}}-K_1\frac{\partial^2\ddot{w}_0}{\partial x^2}-K_3\frac{\partial\ddot{\varphi}}{\partial x}\Big)\delta w_0+\Big(c_2\Big(\frac{\partial P_{xx}}{\partial x}-3R_x\Big)-c_1\Big(\frac{\partial S_{xx}}{\partial x}-Q_g\Big)\\&+K_3\frac{\partial\ddot{w}_0}{\partial x}+K_2\ddot{\varphi}\Big)\delta\varphi\Big)\mathrm{d}x\mathrm{d}t+\int_0^T\Big(\Big(c_0\frac{\partial M_{xx}}{\partial x}+c_2\Big(\frac{\partial P_{xx}}{\partial x}-3R_x\Big)\\&+(1-c_0)Q_x+K_1\frac{\partial\ddot{w}_0}{\partial x}+K_3\ddot{\varphi}\Big)\delta w_0-(c_0M_{xx}+c_2P_{xx})\frac{\partial\delta\dot{w}_0}{\partial x}\\&+(c_1S_{xx}-c_2P_{xx})\delta\varphi\Big)\Big|_0^L\mathrm{d}t.\end{aligned}\tag{13}$$

The force and moment resultants M_{xx}, P_{xx}, S_{xx}, Q_x, Q_g, and R_x can be defined by

$$\begin{cases} \begin{pmatrix} M_{xx} \\ P_{xx} \\ S_{xx} \end{pmatrix} = \int_{-h/2}^{h/2} \sigma_{xx} \begin{pmatrix} z \\ z^3 \\ e(z) \end{pmatrix} \mathrm{d}z \\ \qquad\qquad = \begin{pmatrix} D_{11} & F_{11} & E_{11}^1 \\ F_{11} & H_{11} & E_{11}^2 \\ E_{11}^1 & E_{11}^2 & E_{11}^3 \end{pmatrix} \begin{pmatrix} \varepsilon_{xx}^{(1)} \\ \varepsilon_{xx}^{(3)} \\ \varepsilon_{xx}^{e} \end{pmatrix} - \begin{pmatrix} M_{11}^m \\ P_{11}^m \\ S_{11}^m \end{pmatrix}, \\ \begin{pmatrix} Q_x \\ R_x \\ Q_g \end{pmatrix} = \int_{-h/2}^{h/2} \sigma_{xz} \begin{pmatrix} 1 \\ z^2 \\ g(z) \end{pmatrix} \mathrm{d}z = \begin{pmatrix} A_{55} & D_{55} & E_{55}^1 \\ D_{55} & F_{55} & E_{55}^2 \\ E_{55}^1 & E_{55}^2 & E_{55}^3 \end{pmatrix}, \end{cases} \tag{14}$$

and the mass inertia is expressed as

$$\begin{pmatrix} K_1 \\ K_2 \\ K_3 \end{pmatrix} = \int_{-h/2}^{h/2} \rho \begin{pmatrix} f_1^2 \\ f_2^2 \\ f_1 f_2 \end{pmatrix} \mathrm{d}z = \begin{pmatrix} c_0^2 I_2 + 2c_0 c_2 I_4 + c_2^2 I_6 \\ c_1^2 I_{ee} - 2c_1 c_2 I_{eee} + c_2^2 I_6 \\ -c_0 c_1 I_e - c_1 c_2 I_{eee} + c_0 c_2 I_4 + c_2^2 I_6 \end{pmatrix}, \tag{15}$$

in which

$$(I_0,\, I_2,\, I_4,\, I_6,\, I_e,\, I_{ee},\, I_{eee}) = \int_{-h/2}^{h/2} \rho(1,\, z^2,\, z^4,\, z^6,\, ze(z),\, (e(z))^2,\, z^3 e(z))\mathrm{d}z, \tag{16}$$

where ρ is the mass density, and

$$\begin{cases} \begin{pmatrix} M_{11}^m \\ P_{11}^m \\ S_{11}^m \end{pmatrix} k_{\mathrm{c}} c(t) \sum_{k=s} \int_{z_k}^{z_{k+1}} \overline{q}_{31} \begin{pmatrix} z \\ z^3 \\ e(z) \end{pmatrix} H_z \mathrm{d}z \\ = \begin{pmatrix} \beta \\ \varepsilon \\ \gamma \end{pmatrix} \dfrac{\partial w_0}{\partial t}, \quad s = m, k-m+1, \\ (D_{11},\, F_{11},\, H_{11},\, E_{11}^1,\, E_{11}^2,\, E_{11}^3) \\ = \displaystyle\int_{-h/2}^{h/2} \overline{Q}_{11}^{(k)} (z^2,\, z^4,\, z^6,\, ze(z),\, z^3 e(z),\, (e(z))^2)\mathrm{d}z, \\ (A_{55},\, D_{55},\, F_{55},\, E_{55}^1,\, E_{55}^2,\, E_{55}^3) \\ = \displaystyle\int_{-h/2}^{h/2} \overline{Q}_{55}^{(k)} (1,\, z^2,\, z^4,\, g(z),\, z^2 g(z),\, (g(z))^2)\mathrm{d}z. \end{cases} \tag{17}$$

The governing equations of motion can be written as

$$\begin{aligned} &- c_0 \frac{\partial^2 M_{xx}}{\partial x^2} - c_2 \left(\frac{\partial^2 P_{xx}}{\partial x^2} - 3 \frac{\partial R_x}{\partial x} \right) - (1 - c_0) \frac{\partial Q_x}{\partial x} - q + E_{\mathrm{f}} \\ &- K_1 \frac{\partial^2 \ddot{w}_0}{\partial x^2} - K_3 \frac{\partial \ddot{\varphi}}{\partial x} + I_0 \ddot{w}_0 = 0, \end{aligned} \tag{18}$$

$$c_2 \left(\frac{\partial P_{xx}}{\partial x} - 3R_x \right) - c_1 \left(\frac{\partial S_{xx}}{\partial x} - Q_{gx} \right) + K_3 \frac{\partial \ddot{w}_0}{\partial x} + K_2 \ddot{\varphi} = 0. \tag{19}$$

4 Solution of the problem

By substituting Eqs. (14)–(17) into Eqs. (18) and (19), the dynamic system becomes

$$\begin{aligned}
&c_0(c_0D_{11}+c_2F_{11})\frac{\partial^4 w_0}{\partial x^4}+c_2(c_0F_{11}+c_2H_{11})\Big(\frac{\partial^4 w_0}{\partial x^4}+\frac{\partial^3\varphi}{\partial x^3}\Big)\\
&-c_1(c_0E_{11}^1-c_2E_{11}^2)\frac{\partial^3\varphi}{\partial x^3}+((1-c_0)(6c_2D_{55}-(1-c_0)A_{55})\\
&-9c_2^2F_{55})\frac{\partial^2 w_0}{\partial x^2}+((1-c_0)(3c_2D_{55}-c_1E_{55}^1)-3c_2(3c_2F_{55}-c_1E_{55}^2))\frac{\partial\varphi}{\partial x}\\
&-q+E_{\rm f}+(c_0\beta+c_2\varepsilon)\frac{\partial^2\dot w_0}{\partial x^2}-K_1\frac{\partial^2\ddot w_0}{\partial x^2}-K_3\frac{\partial\ddot\varphi}{\partial x}+I_0\ddot w_0=0, \qquad (20)\\
&c_0(c_2F_{11}-c_1E_{11}^1)\frac{\partial^3 w_0}{\partial x^3}+c_2(c_2H_{11}-c_1E_{11}^2)\Big(\frac{\partial^3 w_0}{\partial x^3}+\frac{\partial^2\phi}{\partial x^2}\Big)\\
&-c_1(c_2E_{11}^2-c_1E_{11}^3)\frac{\partial^2\varphi}{\partial x^2}+(1-c_0)(3c_2D_{55}-c_1E_{55}^1)\frac{\partial w_0}{\partial x}\\
&-3c_2(c_1E_{55}^2-3c_2F_{55})\Big(\varphi+\frac{\partial w_0}{\partial x}\Big)-c_1(3c_2E_{55}^2-c_1E_{55}^3)\varphi\\
&+(c_2\varepsilon-c_1\gamma)\frac{\partial\dot w_0}{\partial x}+K_3\frac{\partial\ddot w_0}{\partial x}+K_2\ddot\varphi=0. \qquad (21)
\end{aligned}$$

These equations can be expanded to any of used four theories. To solve the system, the analytical Navier's method is used with the following simply-supported boundary conditions:

$$w=\varphi=M_{xx}=P_{xx}=S_{xx}=0 \quad \text{at} \quad x=0,L. \qquad (22)$$

The solution takes the following form:

$$\begin{cases} w_0(x,t)=W(t)\sin\dfrac{n\pi x}{L},\\ \varphi(x,t)=X(t)\cos\dfrac{n\pi x}{L},\\ q(x,t)=Q_n(t)\sin\dfrac{n\pi x}{L}. \end{cases} \qquad (23)$$

By using the above equation and Eqs. (20) and (21), the system can be written as

$$\begin{aligned}
&\begin{pmatrix} \widehat{S}_{11} & \widehat{S}_{12}\\ \widehat{S}_{21} & \widehat{S}_{22}\end{pmatrix}\begin{pmatrix} W\\ X\end{pmatrix}+\begin{pmatrix} \widehat{M}_{11} & \widehat{M}_{12}\\ \widehat{M}_{21} & \widehat{M}_{22}\end{pmatrix}\begin{pmatrix} \dot W\\ \dot X\end{pmatrix}\\
&+\begin{pmatrix} \widehat{C}_{11} & \widehat{C}_{12}\\ \widehat{C}_{21} & \widehat{C}_{22}\end{pmatrix}\begin{pmatrix} \ddot W\\ \ddot X\end{pmatrix}=\begin{pmatrix} Q_n\\ 0\end{pmatrix}. \qquad (24)
\end{aligned}$$

We put $q=0$ in Eq. (20) for vibration control. The solution of Eq. (24) takes the following form:

$$(W(t),X(t))=(W_0,X_0)\mathrm{e}^{\lambda_n t}. \qquad (25)$$

The non-trivial solution of Eq. (24) is obtained for all used four theories as

$$\begin{vmatrix} \overline{S}_{11} & \overline{S}_{12}\\ \overline{S}_{21} & \overline{S}_{22}\end{vmatrix}=0, \qquad (26)$$

where

$$\overline{S}_{ij} = \widehat{S}_{ij} + \lambda_n \widehat{M}_{ij} + \lambda_n^2 \widehat{C}_{ij}, \quad i,j = 1,2, \tag{27}$$

in which the coefficients $\widehat{S}_{ij}$, $\widehat{M}_{ij}$, and $\widehat{C}_{ij}$ are given in Appendix B. It is noted that Eq. (26) represents two sets of eigenvalues. The eigenvalues can be expressed by $\lambda_n = -\alpha_n \pm \mathrm{i}\omega_n$. The damping ratio ζ_n of mode n is defined as[50]

$$\zeta_n = \frac{-\alpha_n}{\sqrt{\alpha_n^2 + \omega_n^2}}. \tag{28}$$

Using the following initial conditions (Reddy and Barbosa[5]):

$$\begin{cases} w_0(x,0) = 0, \quad \dot{w}_0(x,0) = 1, \\ \varphi(x,0) = 0, \quad \dot{\varphi}(x,0) = 0, \end{cases} \tag{29}$$

the system solution can be given as

$$w(x,t) = \frac{1}{\omega_n} \mathrm{e}^{-\alpha_n t} \sin(\omega_n t) \, \sin \frac{n\pi x}{L}. \tag{30}$$

In addition, the actuation stress is

$$\sigma_{\mathrm{d}} = -\frac{\overline{q}_{31} k_{\mathrm{c}} c(t)}{\omega_n} (\omega_n \cos(\omega_n t) - \alpha_n \sin(\omega_n t)) \mathrm{e}^{-\alpha_n t} \, \sin \frac{n\pi x}{L}. \tag{31}$$

5 Numerical results and discussion

Here, some numerical results are tabulated to study the dynamic behavior of laminated composite beams with magnetostrictive layers resting on the viscoelastic foundation. Four fiber-reinforced materials which are carbon fiber reinforced polymeric (CFRP), graphite-epoxy (AS/3501) (Gr.-Ep (AS)), glass-epoxy (Gl.-Ep), and born-epoxy (Br.-Ep), are used. Terfenol-D particles embedded in a suitable resin are utilized as magnetostrictive material. The material properties applied are listed in Table 1 as those reported by Reddy and Barbosa[5]. The properties of magnetostrictive material applied are given as $E_{\mathrm{m}} = 26.5\,\mathrm{GPa}$, $\rho_{\mathrm{m}} = 9\,250\,\mathrm{kg{\cdot}m^{-3}}$, $q_{31} = 442.55\,\mathrm{N{\cdot}m^{-1}}$, and $\nu_{\mathrm{m}} = 0$. The length of the beam is equal to 1 m, and its thickness ratio is denoted by $h_\alpha = h/L$. The thickness of fiber-reinforced material layers is denoted by the symbol h_{k}, and the magnetostrictive layer thickness is labeled by the symbol h_{m}. The Euler-Bernoulli's classical, Timoshenko's first-order, Reddy's third-order, and simple shear deformation beam theories are used to predict the deflection damping characteristics. In addition, some numerical results are displayed to observe the behavior of damping coefficients, damped natural frequencies, maximum deflection, vibration damping time, and damping ratio. The effects of different parameters on damping tendencies such as modes, lamination schemes, material properties, positions of magnetostrictive layers from the mid-plane axis, thickness ratio, magnitude of the feedback coefficient, and viscoelastic foundation parameters are investigated. Cross-ply and balanced laminated composite beams are investigated as special cases.

The most natural extension to Winkler's model is Pasternak's model, which connects the spring ends to the shear layer. The present beam rests on a homogeneous three-parameter visco-elastic foundation. The foundation model is characterized by the viscoelastic medium damping coefficient, Pasternak's foundation parameter and linear Winkler's parameter. For the analysis of a structure resting on the pure elastic foundation, the viscosity part is omitted by setting $c_{\mathrm{d}} = 0$. Visco-Winkler's medium is modeled by putting K_{P} equal to zero. For the purpose of completeness and comparisons, firstly, the damping and frequency parameters are

displayed in absence of three-parameter foundation for the laminated composite beam with lamination scheme $[\pm 45/m/0/90]_{\mathrm{s}}$. The damping and frequency parameters are listed in Table 2 for transverse modes $n = 1, 2, \cdots, 5$ according to the simple sinusoidal shear deformation beam theory. The new outcomes are compared with the results obtained by Krishna et al.[4] and Reddy and Barbosa[5]. It is observed that the results given by the three theories ECBT, TFBT, RHBT are relatively different from those of the fourth one, SSBT, in the higher modes only. Moreover, the faster vibration suppression occurs in the higher modes. In the presence of three-parameter viscoelastic medium, the damping and frequency parameters of laminated composite beam with lamination scheme $[\pm 45/m/0/90]_{\mathrm{s}}$ are displayed in Table 3 for transverse modes $n = 1, 2, \cdots, 5$ based on the four theories: ECBT, TFBT, RHBT, and SSBT. It can be observed that the presence of three-parameter foundation gives the largest eigenfrequency parameters, and thus the three-parameter foundation helps to stabilize the system and improve the deflection damping characteristics of the structure. Further, the damping and frequency parameters are directly proportional to the viscoelastic foundation effect.

As a special example, two lamination schemes are analyzed, which are the magnetostrictive sandwich beam with fiber-reinforced core layer and the fiber-reinforced laminated composite beam with magnetostrictive core to illustrate the effects of the thickness ratio and magnetostrictive layer location on the behavior of the eigenfrequency parameters, maximum deflection, vibration suppression time, and damping ratio. The numerical values of all the previous parameters are listed in Table 4. According to the results with the presence of the velocity feedback gain and the foundation effect, the best vibration suppression process occurs whenever the magnetostrictive layers are moved far away from the structure center (see Table 7). Moreover, it is noticeable that the time taken to damp deflection is long whenever the thickness ratio value is low. The effect of the thickness ratio on the vibration damping behavior is also shown in Fig. 2. In addition, the effects of foundation parameters are investigated with and without the velocity feedback gain effect in detail. The damping and frequency parameters, maximum deflection, vibration suppression time, and damping ratio are displayed in Tables 5 and 6. It is observed that the parameters of the foundation $(K_{\mathrm{W}}, K_{\mathrm{P}}, c_{\mathrm{d}})$ may have an almost unnoticeable effect on the controlled motion as the value of the feedback gain coefficient increases. However, the maximum frequency appears when the structure is supported by Pasternak's elastic medium in the uncontrolled motion and without the viscosity term. Winkler's foundation has few effects than Pasternak's medium on frequencies of the smart structures. The damping parameter c_{d} plays an important role in reducing vibration of the structure in absence of the velocity feedback gain coefficient, and this effect also increases as the viscosity coefficient increases (see Figs. 3 and 4).

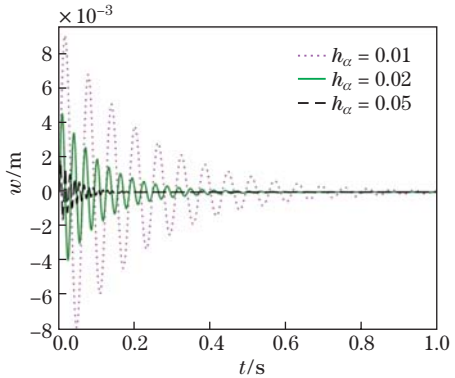

Fig. 2 Center displacement versus time for lay-up $[45/m/-45/0/90]_{\mathrm{s}}$, $n = 1$, $c(t)k_{\mathrm{c}} = 10^4$, $K_{\mathrm{W}} = 50$, $K_{\mathrm{P}} = 10$, and $c_{\mathrm{d}} = \mathrm{e}^{1.5}$ using SSBT for various thickness ratios (color online)

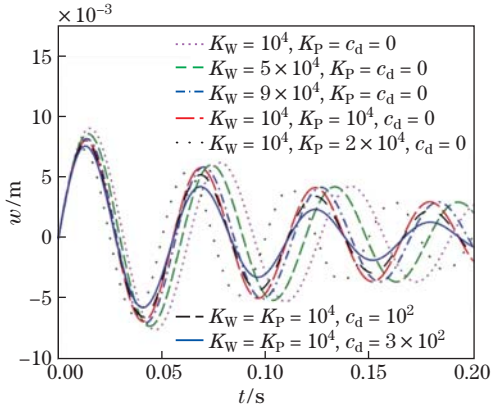

Fig. 3 Effect of foundation parameters on controlled motion of the lay-up $[m/\pm 45/0/90]_s$ at the midpoint using TFBT ($n = 1$, $h_\alpha = 0.01$, and $c(t)k_c = 10^4$) (color online)

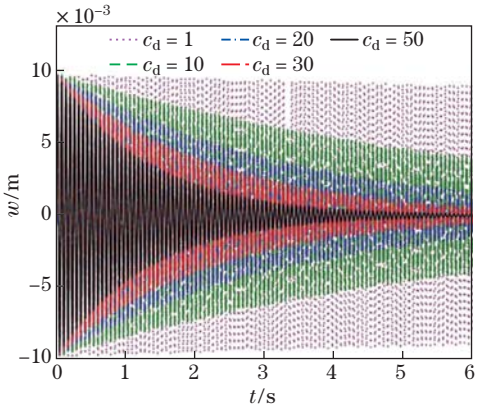

Fig. 4 Effect of viscosity parameters on uncontrolled motion of the lay-up $[45/m/-45/0/90]_s$ at the midpoint using SSBT ($n = 1$, $h_\alpha = 0.01$, $K_W = 50$, and $K_P = 10$ (color online))

Table 1 The properties of fiber-reinforced materials

Material	E_{11}/ GPa	E_{22}/ GPa	G_{12}/ GPa	G_{13}/ GPa	G_{23}/ GPa	ν_{12}	ρ/ (kg·m^{-3})
CFRP	138.6	8.27	4.12	$0.6E_{22}$	$0.6E_{22}$	0.26	1 824
Gr.-Ep (AS)	137.9	8.96	7.10	7.10	6.21	0.3	1 450
Br.-Ep	206.9	20.69	6.9	6.9	4.14	0.3	1 950
Gl.-Ep	53.78	17.93	8.96	8.96	3.45	0.25	1 900

Table 2 Damping and frequency parameters $-\alpha_n \pm \omega_n$ (rad·s^{-1}) for lay-up $[\pm 45/m/0/90]_s$ ($h_\alpha = 0.01$, $K_P = K_W = c_d = 0$, and $c(t)k_c = 10^4$)

Mode	Krishna et al.[4]	ECBT[5]	TFBT[5]	RHBT[5]	SSBT
1	3.29±104.88	3.30±104.85	3.30±104.82	3.30±104.82	3.30±104.87
2	13.19±419.50	13.20±419.37	13.17±418.90	13.16±418.80	13.20±19.05
3	29.70±943.88	29.68±943.40	29.53±941.05	29.48±940.52	29.68±941.20
4	52.89±1 678.83	52.73±1 676.72	52.27±1 669.32	52.10±1 667.68	52.74±1 669.12
5	82.59±2 621.87	82.34±2 619.02	81.22±2 601.04	80.80±2 597.09	82.35±2 599.81

Table 3 Damping and frequency parameters of the transverse modes $-\alpha_n \pm \omega_n$ (rad·s^{-1}) for lay-up $[\pm 45/m/0/90]_s$ ($K_W = e^2, K_P = 6.5, c_d = 2e^{1.5}, c(t)k_c = 10^4$, and $h_\alpha = 0.01$)

Mode	ECBT	TFBT	RHBT	SSBT
1	3.43±104.91	3.43±104.86	3.43±104.88	3.43±104.88
2	13.33±419.59	13.30±419.13	13.29±419.02	13.33±419.06
3	29.81±943.90	29.67±943.55	29.61±943.02	29.81±941.21
4	52.87±1 677.62	52.40±1 670.20	52.23±1 668.55	52.87±1 669.13
5	82.48±2 620.41	81.35±2 602.40	80.93±2 598.42	82.48±2 599.81

Table 4 Damping and frequency parameters, maximum deflection $W_{\max}$(mm), vibration suppression time and damping ratio of two kind lamination schemes ($n = 1, c(t)k_{\rm c} = 10^4, K_{\rm W} = {\rm e}^2, K_{\rm P} = 6.5$, and $c_{\rm d} = 2{\rm e}^{1.5}$)

Lamination	h_α	Theory	$-\alpha_1 \pm \omega_1$	$W_{\max}$	t/s	$\zeta_1/10^{-2}$
$[\pm 45/0/90/m]_{\rm s}$	0.01	ECBT	0.795±116.306	8.598	2.895	0.684
		TFBT	0.795±116.267	8.601	2.897	0.684
		RHBT	0.795±116.264	8.601	2.897	0.684
		SSBT	0.795±116.276	8.600	2.895	0.684
	0.02	ECBT	1.387±232.581	4.300	1.660	0.596
		TFBT	1.384±232.263	4.305	1.664	0.596
		RHBT	1.383±232.245	4.306	1.665	0.595
		SSBT	1.387±232.338	4.304	1.660	0.597
	0.05	ECBT	3.323±581.163	1.721	0.693	0.572
		TFBT	3.268±576.261	1.735	0.705	0.567
		RHBT	3.253±575.983	1.736	0.708	0.565
		SSBT	3.323±581.163	1.721	0.693	0.572
$[m/\pm 45/0/90]_{\rm s}$	0.01	ECBT	6.074±98.481	10.154	0.379	6.156
		TFBT	6.071±98.457	10.157	0.379	6.155
		RHBT	6.070±98.440	10.159	0.379	6.154
		SSBT	6.074±98.454	10.157	0.379	6.158
	0.02	ECBT	11.940±196.915	5.078 3	0.193	6.053
		TFBT	11.917±196.722	5.083 3	0.193	6.047
		RHBT	11.906±196.586	5.086 8	0.193	6.045
		SSBT	11.940±196.702	5.083 8	0.193	6.059
	0.05	ECBT	29.624±491.595	2.034 2	0.078	6.015
		TFBT	29.268±488.623	2.046 6	0.079	5.979
		RHBT	29.100±486.555	2.055 3	0.079	5.970
		SSBT	29.627±488.313	2.047 9	0.078	6.056

Table 5 Damping and frequency parameters, maximum deflection $W_{\max}$ (mm), vibration suppression time and damping ratio for lay-up $[m/\pm 45/0/90]_{\rm s}$ for various viscoelastic parameters ($n = 1, c(t)k_{\rm c} = 10^4$, and $h_\alpha = 0.01$)

$K_{\rm W}$	$K_{\rm P}$	$c_{\rm d}$	Theory	$-\alpha_1 \pm \omega_1$	$W_{\max}$	t/s	$\zeta_1/10^{-2}$
10^2	0	0	ECBT	5.939±98.494	10.153	0.388	6.019
			RHBT	5.934±98.452	10.157	0.388	6.017
			SSBT	5.939±98.467	10.156	0.388	6.020
10^4	0	0	ECBT	5.939±100.001	10.000	0.388	5.928
			RHBT	5.934±99.960	10.004	0.388	5.926
			SSBT	5.939±99.974	10.003	0.388	5.930
5×10^4	0	0	ECBT	5.939±105.871	9.445	0.388	5.601
			RHBT	5.934±105.833	9.449	0.388	5.599
			SSBT	5.939±105.846	9.445	0.388	5.601
10^2	10^2	0	ECBT	5.939±98.645	10.137	0.388	6.009
			RHBT	5.934±98.604	10.142	0.388	6.008
			SSBT	5.939±98.618	10.140	0.388	6.011
10^2	10^3	0	ECBT	5.939±99.996	10.000	0.388	5.929
			RHBT	5.934±99.955	10.004	0.388	5.927
			SSBT	5.939±99.970	10.003	0.388	5.930
10^2	10^4	0	ECBT	5.939±112.619	8.879	0.388	5.266
			RHBT	5.934±112.583	8.882	0.388	5.264
			SSBT	5.939±112.596	8.881	0.388	5.267
10^2	10^2	10	ECBT	6.090±98.636	10.138	0.378	6.162
			RHBT	6.085±98.594	10.143	0.378	6.161
			SSBT	6.090±98.609	10.141	0.378	6.164
10^2	10^2	10^2	ECBT	7.449±98.542	10.148	0.309	7.538
			RHBT	7.445±98.501	10.152	0.309	7.537
			SSBT	7.449±98.516	10.151	0.309	7.540
10^2	10^2	2×10^2	ECBT	8.960±98.416	10.161	0.257	9.067
			RHBT	8.956±98.375	10.165	0.257	9.066
			SSBT	8.960±98.390	10.164	0.257	9.069

Table 6 Damping and frequency parameters, maximum deflection $W_{\max}$ (mm), vibration suppression time and damping ratio for lay-up $[m/\pm 45/0/90]_{\rm s}$ for various viscoelastic parameters ($n = 1, c(t)k_{\rm c} = 0$, and $h_\alpha = 0.01$)

$K_{\rm W}$	$K_{\rm P}$	$c_{\rm d}$	Theory	$-\alpha_1 \pm \omega_1$	$W_{\max}$	t/s	$\zeta_1/10^{-2}$
10^2	0	0	ECBT	0±98.672	10.135	–	0
			TFBT	0±98.648	10.137	–	0
			RHBT	0±98.631	10.139	–	0
			SSBT	0±98.646	10.137	–	0
10^2	10^3	0	ECBT	0±100.172	9.983	–	0
			TFBT	0±100.148	9.985	–	0
			RHBT	0±100.131	9.987	–	0
			SSBT	0±100.146	9.985	–	0
10^2	0	$e^{1.5}$	ECBT	0.068±98.672	10.135	34.008	0.068 6
			TFBT	0.068±98.648	10.137	34.008	0.068 6
			RHBT	0.068±98.631	10.139	34.008	0.068 6
			SSBT	0.068±98.646	10.137	34.008	0.068 6
10^2	0	$89e^{1.5}$	ECBT	6.026±98.488	10.153	0.382	6.107 0
			TFBT	6.026±98.464	10.156	0.382	6.108 0
			RHBT	6.026±98.447	10.158	0.382	6.109 0
			SSBT	6.026±98.462	10.156	0.382	6.109 0
10^2	10^3	$e^{1.5}$	ECBT	0.068±100.172	9.983	34.008	0.067 6
			TFBT	0.068±100.148	9.985	34.008	0.067 6
			RHBT	0.068±100.131	9.987	34.008	0.067 6
			SSBT	0.068±100.146	9.985	34.008	0.067 6
10^2	10^3	$89e^{1.5}$	ECBT	6.026±99.991	10.000	0.382	6.016 0
			TFBT	6.026±99.967	10.003	0.382	6.017 0
			RHBT	6.026±99.950	10.005	0.382	6.018 0
			SSBT	6.026±99.964	10.004	0.382	6.017 0

Table 7 Damping and frequency parameters $-\alpha_1 \pm \omega_1$ (rad·s^{-1}) for different laminates ($n = 1, K_{\rm W} = e^2$, $K_{\rm P} = 6.5, c_{\rm d} = 2e^{1.5}, c(t)k_{\rm c} = 10^4$, and $h_\alpha = 0.01$)

Lamination	ECBT	TFBT	RHBT	SSBT
$[\pm 45/0/90/m]_{\rm s}$	0.795±116.306	0.795±116.269	0.795±116.264	0.795±116.276
$[\pm 45/0/m/90]_{\rm s}$	2.115±116.908	2.114±116.867	2.113±116.862	2.115±116.875
$[\pm 45/m/0/90]_{\rm s}$	3.435±104.914	3.433±104.885	3.432±104.879	3.435±104.881
$[45/m/-45/0/90]_{\rm s}$	4.755±102.206	4.752±102.179	4.751±102.168	4.755±102.168
$[m/\pm 45/0/90]_{\rm s}$	6.074±98.481	6.071±98.457	6.070±98.440	6.074±98.454
$[m/90_4]_{\rm s}$	6.074±70.190	6.073±70.181	6.072±70.177	6.074±70.172
$[m/90/0/90/0]_{\rm s}$	6.074±99.138	6.071±99.114	6.070±99.095	6.074±99.111
$[m/0_4]_{\rm s}$	6.074±143.570	6.068±143.495	6.065±143.439	6.074±143.530

The effect of magnetostrictive layer position on vibration suppression process is investigated with/without velocity feedback gain effect using the four used theories. It is noticeable that in absence of the control gain coefficient, the damping characteristics of beam resting on viscoelastic foundation are better whenever the magnetostrictive layers are placed near the center of the structure (in the z-direction), while the opposite occurs in the presence of velocity feedback gain effect (for more details see Table 7 and Fig. 5). In addition, the controlled motion of two

beam special cases which are cross-ply and balanced laminated composite beams, is carried out. It is found that the beam with lamination scheme $[m/0_4]_s$ represents the strongest beam where it has the largest damping value of deflection. Also, the beam with lamination scheme $[m/\theta^\circ/-\theta^\circ/\theta^\circ/-\theta^\circ]_s$, $\theta = 30$ considers the weakest beam among all cases. Comparison of the fibers-oriented influence on controlled motion for the stacking sequence $[m/\theta^\circ/-\theta^\circ/\theta^\circ/-\theta^\circ]_s$ is shown in Fig. 6 as well as in Fig. 7 to illustrate the deflection damping characteristics for various smart sandwich laminate cases. Generally, the vibration suppression characteristics of general angle-ply, cross-ply and balanced composite laminates are found to be similar.

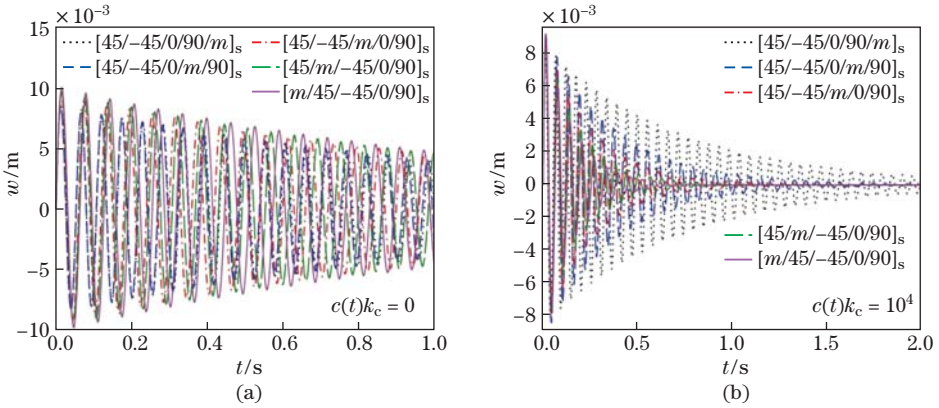

Fig. 5 Effects of smart layer locations on center displacement using SSBT (a) without and (b) with velocity feedback gain effect ($n = 1$, $h_\alpha = 0.01$, $K_W = 50$, $K_P = 10$, and $c_d = 50$) (color online)

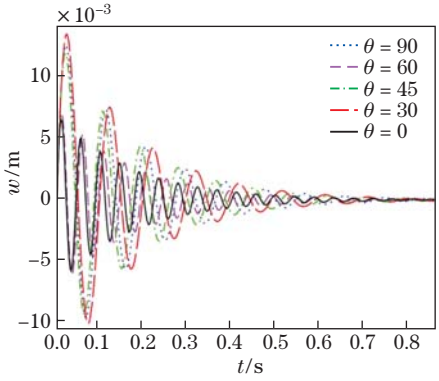

Fig. 6 The center displacement versus time for lay-up $[m/\theta^\circ/-\theta^\circ/\theta^\circ/-\theta^\circ]_s$, $n = 1$, $h_\alpha = 0.01$, $c(t)k_c = 10^4$, $K_W = 100$, $K_P = 20$, $c_d = e^{1.5}$ using TFBT for various orientations (color online)

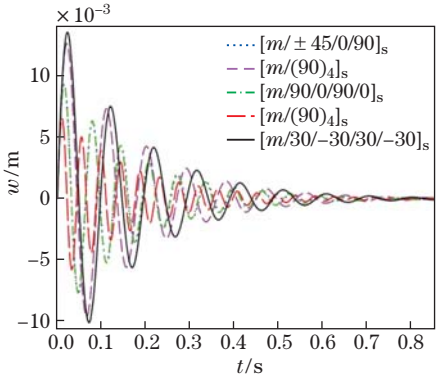

Fig. 7 The deflection damping for various laminates, $n = 1$, $h_\alpha = 0.01$, $c(t)k_c = 10^4$, $K_W = e^2$, $K_P = 6.5$, $c_d = 2e^{1.5}$ at the midpoint by using RHBT (color online)

After studying the effects of the feedback coefficient and material properties of layers on the vibration suppression process, it is noticeable that the materials which have the similar E_1/E_2 value take the same behavior of vibration damping. The deflection suppression characteristics are shown in Fig. 8 for various laminate materials. The symmetric Br.-Ep. laminated beams consider the strongest ones while the Gl.-Ep. laminated beams represent the weakest ones in the present study. Finally, the effects of the feedback coefficient magnitude on vibration

suppression characteristics is shown in Fig. 9. The damping ratio is directly proportional to the magnitude of the feedback coefficient significantly.

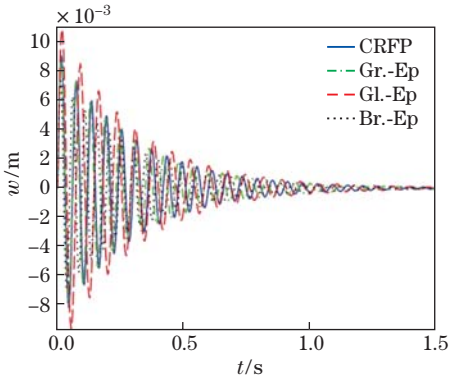

Fig. 8 Effect of material properties on deflection damping for the lay-up $[\pm 45/m/0/90]_{\mathrm{s}}$, $n = 1$, $h_\alpha = 0.01$, $c(t)k_{\mathrm{c}} = 10^4$, $K_{\mathrm{W}} = \mathrm{e}^2$, $K_{\mathrm{P}} = 6.5$, and $c_{\mathrm{d}} = \mathrm{e}^{1.5}$ using ECBT (color online)

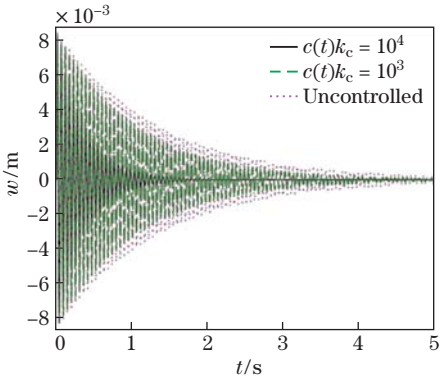

Fig. 9 Effect of feedback coefficient magnitude on center displacement of the lay-up $[\pm 45/0/m/90]_{\mathrm{s}}$, $n = 1$, $h_\alpha = 0.01$, $K_{\mathrm{W}} = 50$, $K_{\mathrm{P}} = 10$, and $c_{\mathrm{d}} = 50$ using RHBT (color online)

6 Conclusions

The present article discusses the vibration of laminated composite beams containing magnetostrictive layers embedded in the three-parameter viscoelastic foundation by using Euler-Bernoulli's classical, Timoshenko's first-order, Reddy's third-order, and simple shear deformation beam theories. The analytical solution of dynamic equations associated with vibration of the current simply-supported laminated composite beam is obtained based on Navier's approach. Terfenol-D magnetostrictive material and velocity feedback control are used in this study to control the vibration of structures. Without the viscosity term, it is observed that the two-parameter Pasternak's foundations have more effects than the one-parameter Winkler's medium on the frequency of the smart structure, in absence of the feedback coefficient $c(t)k_{\mathrm{c}}$. The beam frequency may be vanished when the viscous damping coefficient c_{d} takes high values. In the presence of velocity feedback gain effect, the parameters $(K_{\mathrm{W}}, K_{\mathrm{P}}, c_{\mathrm{d}})$ almost become ineffective at damping time. The damping time and the maximum deflection value are inversely proportional to the magnitude of the feedback coefficient. The vibration damping process is very sensitive to the location of magnetostrictive layers in absence/presence of the feedback coefficient. The balanced, angle-ply, and cross-ply composite laminated beams have the same behavior of the vibration suppression, and the best vibration damping process appears whenever the beams are thicker. According to this study, the present structure can be utilized to improve the smart applications and the control responses of system vibration.

References

[1] REDDY, J. N. *Mechanics of Laminated Composite Plates*: *Theory and Analysis*, CRC Press, Boca Raton (1997)

[2] SUMAN, S. D., HIRWANI, C. K., CHATURVEDI, A., and PANDA, S. K. Effect of magnetostrictive material layer on the stress and deformation behaviour of laminated structure. *IOP Conference Series*: *Materials Science and Engineering*, **178**, 012026 (2017)

[3] KRISHNA, M. A. V., ANJANAPPA, M., and WU, Y. F. The use of magnetostrictive particle actuators for vibration attenuation of flexible beams. *Journal of Sound and Vibration*, **206**(2), 133–149 (1997)

[4] KRISHNA, M. A. V., ANJANAPPA, M., WU, Y. F., BHATTACHARYA, B., and BHAT, M. S. Vibration suppression of laminated composite beam using embedded magnetostrictive layers. *Journal of the Institution of Engineers*: *Aerospace Engineers Journal*, **78**, 38–44 (1998)

[5] REDDY, J. N. and BARBOSA, J. I. On vibration suppression of magnetostrictive beams. *Smart Materials and Structures*, **9**(1), 49–58 (2000)

[6] PRADHAN, S. C., NG, T. Y., LAM, K. Y., and REDDY, J. N. Control of laminated composite plates using magnetostrictive layers. *Smart Materials and Structures*, **10**(4), 1–11 (2001)

[7] SUBRAMANIAN, P. Vibration suppression of symmetric laminated composite beams. *Smart Materials and Structures*, **11**(6), 880–885 (2002)

[8] KUMAR, J. S., GANESAN, N., SWARNAMANI, S., and PADMANABHAN, C. Active control of beam with magnetostrictive layer. *Composite Structures*, **81**(13), 1375–1382 (2003)

[9] KUMAR, J. S., GANESAN, N., SWARNAMANI, S., and PADMANABHAN, C. Active control of cylindrical shell with magnetostrictive layer. *Journal of Sound and Vibration*, **262**(3), 577–589 (2003)

[10] LEE, S. J., REDDY, J. N., and ROSTAM-ABADI, F. Transient analysis of laminated composite plates with embedded smart-material layers. *Finite Elements in Analysis and Design*, **40**(5-6), 463–483 (2004)

[11] KUMAR, J. S., GANESAN, N., SWARNAMANI, S., and PADMANABHAN, C. Active control of simply supported plates with a magnetostrictive layer. *Smart Materials and Structures*, **13**(3), 487–492 (2004)

[12] GHOSH, D. P. and GOPALAKRISHNAN, S. Coupled analysis of composite laminate with embedded magnetostrictive patches. *Smart Materials and Structures*, **14**(6), 1462–1473 (2005)

[13] ZHOU, H. M. and ZHOU, Y. H. Vibration suppression of laminated composite beams using actuators of giant magnetostrictive materials. *Smart Materials and Structures*, **16**(1), 198–206 (2007)

[14] OLABI, A. G. and GRUNWALD, A. Design and application of magnetostrictive materials. *Materials & Design*, **29**(2), 469–483 (2008)

[15] KARUNANIDHI, S. and SINGAPERUMAL, M. Design, analysis and simulation of magnetostrictive actuator and its application to high dynamic servo valve. *Sensors and Actuators A*: *Physical*, **157**(2), 185–197 (2010)

[16] FERREIRA, A. J. M., CARRERA, E., CINEFRA, M., ROQUE, C. M. C., and POLIT, O. Analysis of laminated shells by a sinusoidal shear deformation theory and radial basis functions collocation, accounting for through-the-thickness deformations. *Composites Part B*: *Engineering*, **42**(5), 1276–1284 (2011)

[17] LEE, S. J. and REDDY, J. N. Non-linear response of laminated composite plates under thermomechanical loading. *International Journal of Non-Linear Mechanics*, **40**(7), 971–985 (2005)

[18] REDDY, J. N. On laminated composite plates with integrated sensors and actuators. *Engineering Structures*, **21**(7), 568–593 (1999)

[19] ZENKOUR, A. M. Torsional analysis of heterogeneous magnetic circular cylinder. *Steel and Composite Structures*, **17**(4), 535–548 (2014)

[20] ZHANG, Y., ZHOU, H., and ZHOU, Y. Vibration suppression of cantilever laminated composite plate with nonlinear giant magnetostrictive material layers. *Acta Mechanica Solida Sinca*, **28**, 50–60 (2015)

[21] DAPINO, M. J., FLATAU, A. B., and CALKINS, F. T. Statistical analysis of Terfenol-D materials properties. *Smart Structures and Intelligent Systems*, **3041**, 256–267 (1997)

[22] SUN, L. and ZHENG, X. Numerical simulation on coupling behavior of Terfenol-D rods. *International Journal of Solids and Structures*, **43**(6), 1613–1623 (2006)

[23] ANJANAPPA, M. and BI, J. Modelling, design and control of embedded Terfenol-D actuator. *Smart Structures and Intelligent Systems*, **1917**, 908–918 (1993)

[24] ANJANAPPA, M. and BI, J. A theoretical and experimental study of magnetostrictive mini actuators. *Smart Materials and Structures*, **3**(2), 83–91 (1994)

[25] ZENKOUR, A. M. and EL-SHAHRANY, H. D. Vibration suppression analysis for laminated composite beams contain actuating magnetostrictive layers. *Journal Computational Applied Mechanics*, **50**(1), 69–75 (2019)

[26] ZENKOUR, A. M. and EL-SHAHRANY, H. D. Vibration suppression of advanced plates embedded magnetostrictive layers via various theories. *Journal of Materials Research and Technology*, **9**(3), 4727–4748 (2020)

[27] KOCONIS, D. B., KOLLAR, L. P., and SPRINGER, G. S. Shape control of composite plates and shells with embedded actuators I: voltage specified. *Journal of Composite Materials*, **28**(5), 415–458 (1994)

[28] HONG, C. C. Transient responses of magnetostrictive plates without shear effects. *International Journal of Engineering Science*, **47**(3), 355–362 (2009)

[29] HONG, C. C. Transient responses of magnetostrictive plates by using the GDQ method. *European Journal of Mechanics-A/Solids*, **29**(6), 1015–1021 (2010)

[30] SHANKAR, G., KUMAR, S. K., and MAHATO, P. K. Vibration analysis and control of smart composite plates with delamination and under hygrothermal environment. *Thin-Walled Structures*, **116**, 53–68 (2017)

[31] ARANI, A. G. and MARAGHI, Z. K. A feedback control system for vibration of magnetostrictive plate subjected to follower force using sinusoidal shear deformation theory. *Ain Shams Engineering Journal*, **7**(1), 361–369 (2016)

[32] ARANI, A. G., MARAGHI, Z. K., and ARANI, H. K. Vibration control of magnetostrictive plate under multi- physical loads via trigonometric higher order shear deformation theory. *Journal of Vibration and Control*, **23**(19), 3057–3070 (2017)

[33] CHEN, Y. H., HUANG, Y. H., and SHIH, C. T. Response of an infinite Timoshenko beam on a viscoelastic foundation to a harmonic moving load. *Journal of Sound and Vibration*, **241**(5), 809–824 (2001)

[34] CALIM, F. F. Free and forced vibration analysis of axially functionally graded Timoshenko beams on two-parameter viscoelastic foundation. *Composites Part B*: *Engineering*, **103**, 98–112 (2016)

[35] AREFI, M. and ZENKOUR, A. M. Wave propagation analysis of a functionally graded magneto-electro-elastic nanobeam rest on visco-Pasternak foundation. *Mechanics Research Communications*, **79**, 51–62 (2017)

[36] ZENKOUR, A. M. Nonlocal elasticity and shear deformation effects on thermal buckling of a CNT embedded in a viscoelastic medium. *The European Physical Journal Plus*, **133**, 14 (2018)

[37] SOBHY, M. and ZENKOUR, A. M. Magnetic field effect on thermomechanical buckling and vibration of viscoelastic sandwich nanobeams with CNT reinforced face sheets on a viscoelastic substrate. *Composites Part B*: *Engineering*, **154**, 492–506 (2018)

[38] ZENKOUR, A. M. and AL-SUBHI, A. H. Thermal vibrations of a graphene sheet embedded in viscoelastic medium based on nonlocal shear deformation theory. *International Journal of Acoustics and Vibration*, **24**(3), 485–493 (2019)

[39] BAFERANI, A. H. and SAIDI, A. R. Effects of in-plane loads on vibration of laminated thick rectangular plates resting on elastic foundation: an exact analytical approach. *European Journal of Mechanics-A/Solids*, **42**, 299–314 (2013)

[40] MALEKZADEH, K., KHALILI, S. M. R., and ABBASPOUR, P. Vibration of non-ideal simply supported laminated plate on an elastic foundation subjected to in-plane stresses. *Composite Structures*, **92**(6), 1478–1484 (2010)

[41] THAI, H. T., PARK, M., and CHOI, D. H. A simple refined theory for bending, buckling and vibration of thick plates resting on elastic foundation. *International Journal of Mechanical Sciences*, **73**, 40–52 (2013)

[42] RAZAVI, S. and SHOOSHTARI, A. Free vibration analysis of a magneto-electro-elastic doubly-curved shell resting on a Pasternak-type elastic foundation. *Smart Materials and Structures*, **23**(10), 105003 (2014)

[43] ZAMANI, H. A., AGHDAM, M. M., and SADIGHI, M. Free vibration analysis of thick viscoelastic composite plates on visco-Pasternak foundation using higher-order theory. *Composite Structures*, **182**(12), 25–35 (2017)

[44] ZENKOUR, A. M. Thermal effects on the bending response of fiber-reinforced viscoelastic composite plates using a sinusoidal shear deformation theory. *Acta Mechanica*, **171**(3-4), 171–187 (2004)

[45] ZENKOUR, A. M. On vibration of functionally graded plates according to a refined trigonometric plate theory. *International Journal of Structural Stability and Dynamics*, **5**(2), 279–297 (2005)

[46] ZENKOUR, A. M. The refined sinusoidal theory for FGM plates on elastic foundations. *International Journal of Mechanical Sciences*, **51**(11-12), 869–880 (2009)

[47] ZENKOUR, A. M. Exact relationships between the classical and sinusoidal plate theories for FGM plates. *Mechanics of Advanced Materials and Structures*, **19**(7), 551–567 (2012)

[48] ZENKOUR, A. M. Hygrothermal effects on the bending of angle-ply composite plates using a sinusoidal theory. *Composite Structures*, **94**(12), 3685–3696 (2012)

[49] ZENKOUR, A. M. Trigonometric solution for an exponentially graded thick plate resting on elastic foundations. *Archive of Mechanical Engineering*, **65**(2), 193–208 (2018)

[50] LI, J., MA, Z., WANG, Z., and NARITA, Y. Random vibration control of laminated composite plates with piezoelectric fiber reinforced composites. *Acta Mechanica Solida Sinca*, **29**(3), 316–327 (2016)

Appendix A

The coefficients $\overline{Q}_{ij}^{(k)}$ and $\overline{q}_{ij}$ appearing in Eqs. (5) and (6) are given by

$$
\begin{cases}
\overline{Q}_{11}^{(k)} = Q_{11}^{(k)} \cos^4\theta^{(k)} + 2\left(Q_{12}^{(k)} + 2Q_{66}^{(k)}\right)\cos^2\theta^{(k)}\sin^2\theta^{(k)} + Q_{22}^{(k)}\sin^4\theta^{(k)}, \\
\overline{Q}_{13}^{(k)} = Q_{13}^{(k)} \cos^2\theta^{(k)} + Q_{23}^{(k)}\sin^2\theta^{(k)}, \quad \overline{Q}_{33}^{(k)} = Q_{33}^{(k)}, \\
\overline{Q}_{55}^{(k)} = Q_{55}^{(k)} \cos^2\theta^{(k)} + Q_{44}^{(k)}\sin^2\theta^{(k)}, \\
Q_{11}^{(k)} = \dfrac{1-\nu_{23}^{(k)}\nu_{32}^{(k)}}{E_{22}^{(k)}E_{33}^{(k)}\Delta}, \quad Q_{12}^{(k)} = \dfrac{\nu_{21}^{(k)}+\nu_{31}^{(k)}\nu_{23}^{(k)}}{E_{22}^{(k)}E_{33}^{(k)}\Delta} = \dfrac{\nu_{12}^{(k)}+\nu_{13}^{(k)}\nu_{32}^{(k)}}{E_{11}^{(k)}E_{33}^{(k)}\Delta}, \\
Q_{22}^{(k)} = \dfrac{1-\nu_{13}^{(k)}\nu_{31}^{(k)}}{E_{11}^{(k)}E_{33}^{(k)}\Delta}, \quad Q_{13}^{(k)} = \dfrac{\nu_{31}^{(k)}+\nu_{21}^{(k)}\nu_{32}^{(k)}}{E_{22}^{(k)}E_{33}^{(k)}\Delta} = \dfrac{\nu_{13}^{(k)}+\nu_{12}^{(k)}\nu_{23}^{(k)}}{E_{11}^{(k)}E_{22}^{(k)}\Delta}, \\
Q_{23}^{(k)} = \dfrac{\nu_{32}^{(k)}+\nu_{12}^{(k)}\nu_{31}^{(k)}}{E_{11}^{(k)}E_{33}^{(k)}\Delta} = \dfrac{\nu_{32}^{(k)}+\nu_{21}^{(k)}\nu_{13}^{(k)}}{E_{11}^{(k)}E_{33}^{(k)}\Delta}, \quad Q_{33}^{(k)} = \dfrac{1-\nu_{12}^{(k)}\nu_{21}^{(k)}}{E_{11}^{(k)}E_{22}^{(k)}\Delta}, \\
Q_{44}^{(k)} = G_{23}^{(k)}, \quad Q_{55}^{(k)} = G_{31}^{(k)}, \quad Q_{66}^{(k)} = G_{12}^{(k)}, \\
\Delta = \dfrac{1-\nu_{12}^{(k)}\nu_{21}^{(k)}-\nu_{23}^{(k)}\nu_{32}^{(k)}-\nu_{13}^{(k)}\nu_{31}^{(k)}-2\nu_{21}^{(k)}\nu_{13}^{(k)}\nu_{32}^{(k)}}{E_{11}^{(k)}E_{22}^{(k)}E_{33}^{(k)}}, \\
\nu_{21}^{(k)} = \dfrac{\nu_{12}^{(k)}E_{22}^{(k)}}{E_{11}^{(k)}}, \quad \nu_{31}^{(k)} = \dfrac{\nu_{13}^{(k)}E_{33}^{(k)}}{E_{11}^{(k)}}, \quad \nu_{32}^{(k)} = \dfrac{\nu_{23}^{(k)}E_{33}^{(k)}}{E_{22}^{(k)}}, \\
\overline{q}_{31} = q_{31}\cos^2\theta + q_{32}\sin^2\theta, \quad \overline{q}_{32} = q_{32}\cos^2\theta + q_{31}\sin^2\theta, \\
\overline{q}_{36} = (q_{31}-q_{32})\sin\theta\cos\theta, \quad \overline{q}_{14} = (q_{15}-q_{24})\sin\theta\cos\theta, \\
\overline{q}_{24} = q_{24}\cos^2\theta + q_{15}\sin^2\theta, \quad \overline{q}_{15} = q_{15}\cos^2\theta q_{24}\sin^2\theta, \\
\overline{q}_{25} = (q_{15}-q_{24})\sin\theta\cos\theta,
\end{cases}
$$

where E_{ii} are Young's moduli in the material principal directions, ν_{ij} are Poisson's ratios, G_{ij} are the shear moduli, and q_{ij} represent the magnetostrictive moduli.

Appendix B

The components of the coefficients $\widehat{S}_{ij}$, $\widehat{M}_{ij}$, and $\widehat{C}_{ij}$ $(i = 1, 2)$ appearing in Eq. (25) can be expressed as

$$\begin{cases} \widehat{S}_{11} = (c_0^2 D_{11} + 2c_0c_2F_{11} + c_2^2H_{11})\Big(\dfrac{n\pi}{L}\Big)^4 + ((1-c_0)((1-c_0)A_{55} - 6c_2D_{55}) \\ \qquad + 9c_2^2F_{55} + K_{\mathrm{P}})\Big(\dfrac{n\pi}{L}\Big)^2 + K_{\mathrm{W}}, \\ \widehat{S}_{12} = \widehat{S}_{21} = (c_0(c_2F_{11} - c_1E_{11}^1) + c_2(c_2H_{11} - c_1E_{11}^2))\Big(\dfrac{n\pi}{L}\Big)^3 \\ \qquad + ((1-c_0)(c_1E_{55}^1 - 3c_2D_{55}) + 3c_2(3c_2F_{55} - c_1E_{55}^2))\dfrac{n\pi}{L}, \\ \widehat{S}_{22} = (c_2^2H_{11} + c_1(c_1E_{11}^3 - 2c_2E_{11}^2))\Big(\dfrac{n\pi}{L}\Big)^2 + 3c_2(3c_2F_{55} - 2c_1E_{55}^2) - c_1^2E_{55}^3, \\ \widehat{M}_{11} = -(c_0\beta + c_2\varepsilon)\Big(\dfrac{n\pi}{a}\Big)^2 + c_{\mathrm{d}}, \quad \widehat{M}_{12} = \widehat{M}_{22} = 0, \quad \widehat{C}_{22} = K_2, \\ \widehat{M}_{21} = (c_1\gamma - c_2\varepsilon)\dfrac{n\pi}{L}, \quad \widehat{C}_{11} = K_1\Big(\dfrac{n\pi}{L}\Big)^2 + I_0, \quad \widehat{C}_{12} = \widehat{C}_{21} = K_3\dfrac{n\pi}{L}. \end{cases}$$

For the ECBT $(c_0 = 1, c_1 = c_2 = 0)$,

$$\begin{cases} \widehat{S}_{11} = D_{11}\Big(\dfrac{n\pi}{L}\Big)^4 + K_{\mathrm{P}}\Big(\dfrac{n\pi}{L}\Big)^2 + K_{\mathrm{W}}, \quad \widehat{M}_{11} = -\beta\Big(\dfrac{n\pi}{L}\Big)^2 + c_{\mathrm{d}}, \\ \widehat{C}_{11} = I_2\Big(\dfrac{n\pi}{L}\Big)^2 + I_0. \end{cases}$$

For the TFBT $(c_0 = 0, c_1 = 1, c_2 = 0)$,

$$\begin{cases} \widehat{S}_{11} = A_{55}\Big(\dfrac{n\pi}{L}\Big)^4 + K_{\mathrm{P}}\Big(\dfrac{n\pi}{L}\Big)^2 + K_{\mathrm{W}}, \quad \widehat{S}_{12} = E_{55}^1\dfrac{n\pi}{L}, \\ \widehat{S}_{22} = E_{11}^3\Big(\dfrac{n\pi}{L}\Big)^2 - E_{55}^3, \quad \widehat{M}_{11} = c_{\mathrm{d}}, \quad \widehat{M}_{21} = \gamma\dfrac{n\pi}{L}, \quad \widehat{C}_{11} = I_0, \quad \widehat{C}_{22} = I_{ee}. \end{cases}$$

For the RHBT $(c_0 = 0, c_1 = 1, c_2 = \frac{4}{3h^2})$,

$$\begin{cases} \widehat{S}_{11} = H_{11}\Big(\dfrac{4}{3h^2}\Big)^2\Big(\dfrac{n\pi}{L}\Big)^4 + \Big(A_{55} - \dfrac{4}{h^2}\Big(2D_{55} + \dfrac{4}{h^2}F_{55}\Big) + K_{\mathrm{P}}\Big)\Big(\dfrac{n\pi}{L}\Big)^2 + K_{\mathrm{W}}, \\ \widehat{S}_{12} = \dfrac{4}{3h^2}\Big(\dfrac{4}{3h^2}H_{11} - E_{11}^2\Big)\Big(\dfrac{n\pi}{L}\Big)^3 - \Big(\dfrac{4}{h^2}\Big(D_{55} + E_{55}^2 - \dfrac{4}{h^2}F_{55}\Big) - E_{55}^1\Big)\dfrac{n\pi}{L}, \\ \widehat{S}_{22} = \Big(\dfrac{4}{3h^2}\Big(\dfrac{4}{3h^2}H_{11} - 2E_{11}^2\Big) + E_{11}^3\Big)\Big(\dfrac{n\pi}{L}\Big)^2 + \dfrac{4}{h^2}\Big(2E_{55}^2 - \dfrac{4}{h^2}F_{55}\Big) - E_{55}^3, \\ \widehat{M}_{11} = -\dfrac{4\varepsilon}{3h^2}\Big(\dfrac{n\pi}{L}\Big)^2 + c_{\mathrm{d}}, \quad \widehat{M}_{21} = \Big(\gamma - \dfrac{4\varepsilon}{3h^2}\Big)\dfrac{n\pi}{L}, \\ \widehat{C}_{11} = I_6\Big(\dfrac{4}{3h^2}\Big)^2\Big(\dfrac{n\pi}{L}\Big)^2 + I_0, \quad \widehat{C}_{12} = \dfrac{4}{3h^2}\Big(\dfrac{4}{3h^2}I_6 - I_{eee}\Big)\dfrac{n\pi}{L}, \\ \widehat{C}_{22} = I_{ee} + \dfrac{4}{3h^2}\Big(\dfrac{4}{3h^2}I_6 - I_{eee}\Big). \end{cases}$$

For the SSBT $(c_0 = 1, c_1 = 1, c_2 = 0)$,

$$\begin{cases} \widehat{S}_{11} = D_{11}\Big(\dfrac{n\pi}{L}\Big)^4 + K_{\mathrm{P}}\Big(\dfrac{n\pi}{L}\Big)^2 + K_{\mathrm{W}}, \quad \widehat{S}_{12} = -E_{11}^1\Big(\dfrac{n\pi}{L}\Big)^3, \\ \widehat{S}_{22} = E_{11}^3\Big(\dfrac{n\pi}{L}\Big)^2 - E_{55}^3, \quad \widehat{M}_{11} = -\beta\Big(\dfrac{n\pi}{L}\Big)^2 + c_{\mathrm{d}}, \quad \widehat{M}_{21} = \gamma\dfrac{n\pi}{L}, \\ \widehat{M}_{12} = \widehat{M}_{22} = 0, \quad \widehat{C}_{11} = I_2\Big(\dfrac{n\pi}{L}\Big)^2 + I_0, \quad \widehat{C}_{12} = -I_e\dfrac{n\pi}{L}, \quad \widehat{C}_{22} = I_{ee}. \end{cases}$$